Master's Thesis

Perceptual Analysis and Rendering of Vibrotactile Flows on a Mobile Device

Jongman Seo (서 종 만)

Department of Computer Science and Engineering

Pohang University of Science and Technology

2018

모바일 기기에 적용된 진동 흐름의 인지적 분석 및 렌더링

Perceptual Analysis and Rendering of Vibrotactile Flows on a Mobile Device

Perceptual Analysis and Rendering of Vibrotactile Flows on a Mobile Device

by

Jongman Seo

Department of Computer Science and Engineering

Pohang University of Science and Technology

A thesis submitted to the faculty of the Pohang University of Science and Technology in partial fulfillment of the requirements for the degree of Master of Science in the Computer Science and Engineering

Pohang, Korea

4. 17. 2018

Approved by

Seungmoon Choi

Academic advisor

Perceptual Analysis and Rendering of Vibrotactile Flows on a Mobile Device

Jongman Seo

The undersigned have examined this thesis and hereby certify
that it is worthy of acceptance for a master's degree from
POSTECH

4. 17. 2018

Committee Chair   Seungmoon Choi

Member   Sung H. Han

Member   Hee-Kap Ahn

MCSE   서 종 만. Jongman Seo

20090852   Perceptual Analysis and Rendering of Vibrotactile Flows on a Mobile Device,

모바일 기기에 적용된 진동 흐름의 인지적 분석 및 렌더링

Department of Computer Science and Engineering , 2018, 53p, Advisor : Seungmoon Choi. Text in English.

ABSTRACT

"Vibrotactile flow" refers to a continuously moving sensation of vibrotactile stimulation applied by a few actuators directly onto the skin or through a rigid medium. We first investigates the feasibility of vibrotactile flow using two vibrotactile actuators in a mobile device via psychophysical experiment that employed an open response paradigm. The subjects answered the perceived positions and intensities of vibrotactile sensations by drawing graphs with respect to time. The results demonstrated that such "vibrotactile flow" can be reliably produced in a mobile device and that a performance trade-off exists depending on the vibration rendering method and signal duration used for rendering. We extend this study by investigating the perceptual characteristics of vibrotactile flows rendered on a mobile device and proposing a synthesis framework for vibrotactile flows with desired perceptual properties. Furthermore, we extend the dimension of vibrotactile flows to two dimensions by means of *edge flows*—vibrotactile flows that rotate along the edges of a rectangular mobile device, rendered using four actuators placed at its four corners. We designed 32 edge flows and carried out a longitudi-

nal user study in order to measure the information transmission capacity of edge flows, while looking into the effects of practice and correct-answer feedback on the identification accuracy of edge flows. Results showed that the information transmission capacity of the edge flows was 3.70 bits, which is greater than for most previous studies; that some extent of practice is required for robust identification, but it can take place quickly; and that correct-answer feedback is advantageous but its degree of improvement was less than that of repeated practice.

Contents

I. Introduction

Mobile (or handheld) devices, such as mobile phones, PDAs, portable game players, and portable multimedia players, have deeply permeated our daily life, and have become virtually indispensable. Such devices, however, still have many drawbacks due to the small form factor, and the inconvenience of user interface is a prominent issue. Researchers seeking for means to improve the user interface have focused on incorporating advanced interaction modalities, such as motion sensing [1], haptic feedback [2], and augmented reality [3]. Among these approaches, vibrotactile feedback is most commonly utilized for mobile device interaction. For instance, vibrotactile effects for games, e.g., for collisions and gun fires, have been popular for a long time. Some mobile devices play music along with "vibrotactile music," enhancing the affective experience of a user [4]. Moreover, many recent commercial mobile phones with full touch screens no longer carry a physical keyboard; it is replaced with a virtual keyboard with vibrotactile feedback. Vibrotactile feedback can significantly improve the input accuracy of a virtual keyboard [2].

Despite the popularity of vibrotactile feedback, only one vibrotactile actuator is usually included in a mobile device due to its limited space. This enforces to encode desired information in the temporal variations of a signal, even though the human vibrotactile perception of temporal factors is relatively poor [5]. This problem is particularly apparent when absolute identification of vibrotactile stimuli is required. For example, the maximum information transfer (IT) attained by temporal coding was 1.68 bits ($2^{\text{IT}} = 3.2$ stimuli) when vibration amplitude and frequency were co-varied to provide equal differences in the perceived intensity [6]. The maximum IT was 1.76 bits (3.4 stimuli) even when all amplitude,

frequency, and duration were used as design variables [7]. As such, vibrotactile signals must be designed very carefully, so that they have high discriminability, learnability, and retainability, along with a low attentional requirement. A large number of previous studies were devoted to this topic (see [8] for a review), but fundamental limits still exist for the temporal information coding in terms of the richness of vibrotactile sensations and the amount of information that can be reliably conveyed.

To improve upon this situation, the use of multiple tactile actuators for spatially distributed feedback on a mobile device has received increasing attention [9, 10]. These studies suggested that communicating information through more than four locations is possible to a degree, but the rigid structure of mobile devices disables precise vibration localization unless an additional vibration damping mechanism is used. This leverages the fact that spatial tactile perception is intuitive and naturally maps to the perception of egocentric orientation, thereby providing greater potential for higher-capacity information transfer [11]. This was evidenced by a wristband-type tactile display that used three vibration motors to stimulate three different sites around the wrist [12]. Its IT was as high as 4.28 bits (19.4 stimuli) when measured with 24 spatiotemporal patterns designed by varying starting point, direction, temporal pattern, and intensity. This problem shifted research interest from rendering positional information to directional information, for example, by means of *vibrotactile flows*.

A vibrotactile flow refers to a vibrotactile sensation continuously moving on the surface of a mobile device, rendered using only a few actuators [13, 14, 15]. This can be done with even two distant actuators by controlling their relative actuation timings or intensities. This enables the user to perceive vibrotactile sensations that move from one end to the other end of the device, providing natural directional sense. For example, Kim et al. developed a vibrotactile

flow rendering algorithm that changes the time gap between the outputs of two vibration motors (Eccentric Rotating Masses; ERMs) [13]. We examined the feasibility of vibrotactile flow rendering using two Linear Resonant Actuators (LRAs) by controlling the intensities of their output signals [14]. More recently, Kang et al. presented an improved algorithm in which the excitation frequency of the two amplitude-modulated inputs produced by two wideband piezoelectric actuators is also varied to generate smoother vibrotactile flows on a thin plate [15]. Even a dedicated driver IC for a mobile device was developed for vibrotactile flow rendering [16]. Yatani and Truong also demonstrated a similar flow effect with multiple ERMs embedded on the rear side of a mobile device [17]. These previous studies concur in that vibrotactile flows can be an effective means for delivering vivid directional information on a mobile device. This benefit can be instrumental for some applications, such as tactile navigation aids for the sensory impaired [18].

The perceptual basis of vibrotactile flow can be traced back to the well-known tactile illusions of apparent tactile motion [19] and phantom sensation [20]. When the skin is directly stimulated by two separate vibrotactile actuators, a single vibrotactile sensation can be elicited midway between the two stimulation points. Furthermore, the position of the sensation can be moved between the two stimulation points by controlling the intensities of the two stimuli (amplitude inhibition) or the time gap between the stimuli (temporal inhibition) [20]. A similar effect can also be achieved via electrocutaneous stimulation [21]. These perceptual illusions are quite robust such that they can be used to render continuous sensations on the user's back using a 2D array of tactors [22]. Unlike these earlier studies, in the case of vibrotactile flows, a mobile device works as a solid medium that transmits superimposed vibrotactile signals from two actuators. However, how to control the perceptual quality of vibrotactile flow in a systematic way remains an open question. We investigate the perceptual characteristics of vibrotactile

flows rendered on a mobile device with a goal to find a *synthesis* framework of vibrotactile flows with desired perceptual properties.

A natural extension of 1D vibrotactile flows is those moving on a 2D plane, which we call 2D vibrotactile flows. We explored the feasibility of 2D vibrotactile flows with emphasis on their information transmission capacity.

1.1 Paper Overview

In this thesis, we first demonstrate that such phantom sensations can be robustly elicited in the hand holding a mobile device. Using two voice-coil actuators attached onto a device mockup, we confirmed that linearly moving vibrotactile sensations, i.e., "vibrotactile flows," can be created on the user's palm. A formal psychophysical experiment was then followed in order to quantify the characteristics of the perceived positions and intensities of vibrotactile flows. The experiment was designed in an open response paradigm with three independent factors: vibration rendering method, vibration duration, and sensation movement direction. Note that in haptic perception literature for the phantom sensations, vibrotactile actuators were placed directly on the skin, and were isolated without any physical medium connecting the actuators (e.g., see [23] where two vibration motors were applied on the forearm). In contrast, the mobile device considered in this study works as a solid medium that transmits the superimposed vibrotactile signals of the two actuators to the palm. Therefore, the situations and perceptual consequences can be fundamentally different.

We also investigate the perceptual characteristics of vibrotactile flows rendered on a mobile device with a goal to find a *synthesis* framework of vibrotactile flows with desired perceptual properties. To this end, our framework uses synthesis equations of a general polynomial form. This is based on our earlier finding that the function form of vibration amplitude commands and the duration of

vibration signals affect the perceptual attributes of vibrotactile flow, such as the perceived distance of sensation movement and the smoothness of intensity changes [14]. Using these synthesis equations, we carried out a perceptual experiment to investigate the effects of the synthesis parameters on an expanded set of perceptual variables, including sensation movement distance, sensation velocity variation, sensation intensity variation, and the subjective confidence of flow-like sensation. This procedure led to the derivation of a set of mathematical functions that describe the perceptual characteristics of vibrotactile flows.

Furthermore, we concerned with 2D vibrotactile flows, which elicit tactile sensations moving continuously on a 2D plane. In particular, we study *edge flows*: 2D vibrotactile flows that travel along the edges of a mobile device. Edge flows are a special case of 2D flows, and they can be rendered by combining 1D vibrotactile flows sequentially. This simplicity makes edge flows an adequate first step for 2D vibrotactile flow research. We aimed to quantify the information transmission capacity of edge flows, and to assess the learning effect of edge flows, which was expected to be higher than for 1D flows. We designed 32 edge flows and carried out a longitudinal user study in order to measure the information transmission capacity of edge flows, while looking into the effects of practice and correct-answer feedback on the identification accuracy of edge flows.

II. Initial Study of 1D Vibrotactile Flows

We examined the feasibility of one-dimensional (1D) vibrotactile flow rendering using two Linear Resonant Actuators (LRAs) by controlling the intensities of their output signals. A formal psychophysical experiment was performed in order to quantify the characteristics of the perceived positions and intensities of vibrotactile flows.

2.1 Methods

This section presents the methods used for a human experiment carried out to confirm the feasibility of vibrotactile flow via a handheld device.

2.1.1 Subjects

Ten subjects (20–29 years old with an average of 22.7; eight males and two females) participated in the experiment. All subjects were right-handed and everyday users of a mobile device. No subject reported any known sensorimotor abnormality. Subjects were compensated for their efforts after the experiment.

2.1.2 Apparatus

A mobile device mockup made of acrylic resin (10.5 cm × 4.5 cm × 1.5 cm) shown in Figure 2.1 was used in the experiment. Two Linear Resonant Actuators (LRAs; model MVMU-A360G; LG Innotek) were attached onto one side of the mockup. The LRA is a type of voice-coil actuators which rely on the resonance of mass and spring elements to produce high-intensity vibrations. It is lightweight, small, and has a relatively short rising time (about a few ten ms). Recent mobile phones with full touch screens use an LRA for vibrotactile feedback. The rated
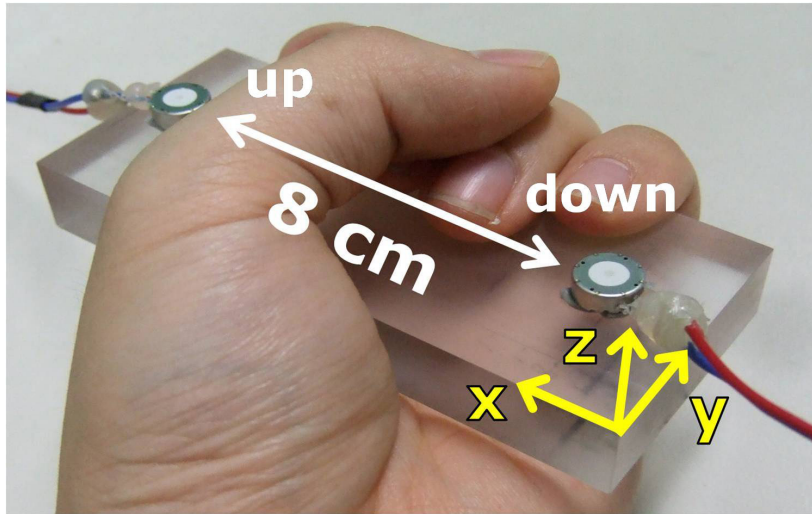
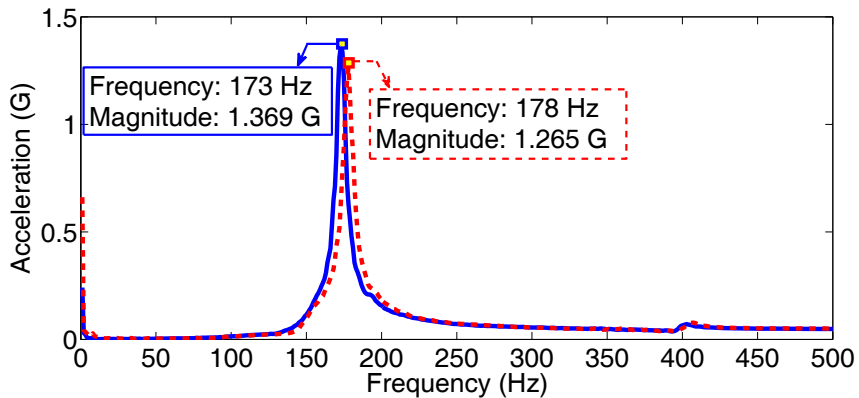Figure 2.1: Handheld mockup used in the experiment.

Figure 2.2: Frequency responses of the two vibrotactile actuators.

voltage of our LRA model is 2.8 V (peak-to-peak) with a nominal resonance frequency of 175 Hz. The two LRAs were powered by a custom-made amplifier that was connected to a PC via a data acquisition card (National Instruments; USB-6251) at a sampling rate of 10 kHz. The distance between the two LRAs was 8 cm throughout the experiment. In pilot experiments, we found that the minimum distance that could produce the sensation of vibrotactile flow was about 2 cm.

In order to determine the frequency of sinusoidal signals to drive the LRAs,

F, we estimated the frequency responses of the two LRAs. Each LRA was driven with sinusoidal voltage waveforms with frequencies in $1 - 500$ Hz. To measure the amplitudes of resulting vibrations, an accelerometer (model 8765A250M5; Kistler) was fastened in the center of the mockup held in the hand. This setup was also used in all other acceleration measurements. The accelerometer responded to vibrations in the z-axis shown Figure 2.1, since it matched the primary vibration direction of the LRAs. As shown in Figure 2.2, the two LRAs exhibited slightly different resonance frequencies (173 and 178 Hz, respectively) and maximum acceleration amplitudes. We selected F such that the minimum of the two response magnitudes at F was the greatest, and $F = 174$ Hz.

We then calibrated the physical intensities of the two LRAs. The amplitudes of vibrations driven with $F = 174$ Hz were measured for each LRA using the accelerometer for 20 amplitude levels of input voltage. The measured input-output relation was inverted for each LRA. This inverted relation was used in the experiment to compute an input voltage that would generate a desired output acceleration.

A phase offset can also exist between two sinusoidal waves produced from the LRAs. The offset reduces the overlapped amplitudes when the two waves are superimposed. Thus, we estimated the phase offset by exhaustively searching the phase difference between two input voltage waveforms that resulted in the largest acceleration output. This phase offset was used in rendering vibrotactile stimuli in the experiment.

2.1.3 Vibration Rendering Algorithms

To create vibrotactile flows, we considered two vibration rendering algorithms. These were adapted from amplitude inhibition algorithms for the phantom sensations originally presented in [20]. Let T be the total time period during

which vibration rendering is applied, and $a_1(t)$ and $a_2(t)$ be the acceleration amplitudes to be produced by the two LRAs at time t, respectively. In linear amplitude rendering, the acceleration amplitude of one LRA was linearly increased over time while that of the other LRA was linearly decreased, such that:

$$a_1(t) = a_{max}\frac{t}{T} \quad \text{and} \quad a_2(t) = a_{max}\left(1 - \frac{t}{T}\right) \tag{2.1}$$

where a_{max} is the maximum acceleration amplitude. In contrast, in log amplitude rendering, the acceleration amplitudes were scaled using logarithm functions:

$$a_1(t) = a_{max}\frac{\log(t+1)}{\log(T+1)} \quad \text{and} \quad a_2(t) = a_{max}\frac{\log(T-t+1)}{\log(T+1)} \tag{2.2}$$

Figure 2.3 illustrates the amplitude characteristics of the two algorithms.

We confirmed in the pilot experiments that both methods can produce the sensations of vibrotactile flows that linearly move from LRA 2 to LRA 1 over time. The goal of this experiment was to identify the quantitative characteristics of the sensations. In the experiment, a_{max} was set to 1.5688 G, and the desired acceleration amplitudes were converted to appropriate input voltage amplitudes using the calibration data described in Section 2.1.2.

2.1.4 Stimuli and Procedures

The experiment had three independent variables. The first variable was the vibration rendering method: linear amplitude rendering and log amplitude rendering. The second variable was the duration of vibrotactile stimulation. We used two values, $T = 4$ and 8 s, which correspond to the nominal velocities of sensation movements of 2 and 1 cm/s, respectively, for the 8-cm distance between the two LRAs. The last variable was the direction of sensation movements: upward and downward. It follows that a total of eight kinds of stimuli were defined by combining the three independent variables.

During the experiment, the subject grasped the handheld mockup with the left hand (see Figure 2.1). The experiment began with a training session in which
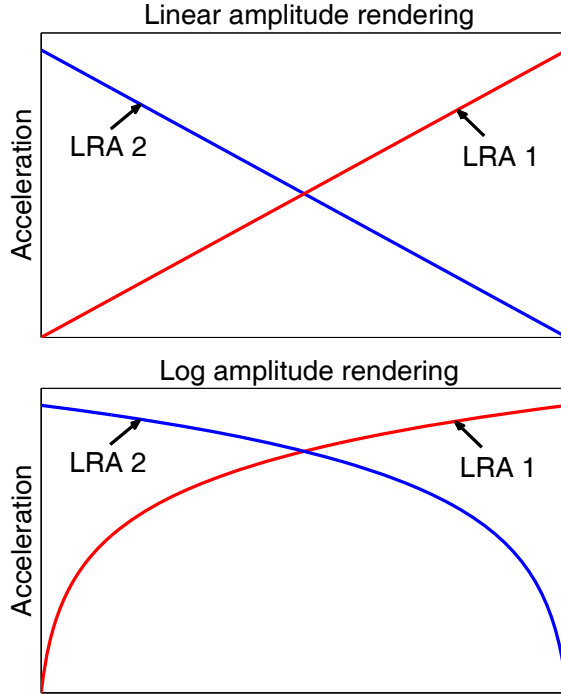
Figure 2.3: Illustration of the two vibrotactile rendering algorithms.

the eight stimuli were presented twice each (total 16 trials) in a randomized order. In a main session, the eight stimuli were presented five times each (total 40 trials). The number of trials was the only difference between the training and main sessions.

In each trial, the subject answered the changing patterns of the perceived intensity and position of a vibrotactile flow with respect to time. To measure the perceived intensity, a reference stimulus was presented first. For this, an LRA at the beginning position of the vibrotactile flow (e.g., in Figure 2.1, the LRA on the top for vibrotactile flows moving downward, and vice versa) was vibrated with a physical intensity of a_{max} for 1 s. Then, the vibrotactile flow was rendered. After this, the subject was asked to draw a graph that depicted the perceived intensity of the vibrotactile flow using the right hand. The graph had seven levels in both relative time and perceived intensity (e.g., see Figure 2.4).

The meanings of the levels were defined as follows. Time levels 0 and 6 indicated the beginning and ending time instants of vibrotactile stimulation, respectively. The subject was instructed to regard intensity level 4 as the perceived intensity of the reference stimulus and intensity level 0 as the level of no vibration, and to scale the perceived intensity of the test stimulus accordingly. After the intensity measurement, the same vibrotactile flow was presented again, but without the reference stimulus, for the measurement of perceived position. The subject was asked to draw another graph for relative time vs. sensation position, both in seven-level scales (e.g., see Figure 2.4). Position levels 0 and 6 were defined as the positions of the LRAs in the bottom and top of the mockup, respectively.

During the experiment, the subjects wore headphones that played white noise to block any auditory cue. It took about an hour to complete the experiment per subject. The subjects could take a break whenever necessary.

2.1.5 Data Analysis

We defined two measures to represent the quality of vibrotactile flows experienced by the subjects. The first measure was to quantify the amount of change in the perceived position. For this, linear regression was applied on each graph of time vs. perceived position, and the absolute value of the slope of a fitted line was taken as the measure (denoted by α). A higher α value indicates that a larger distance was spanned in the perceived position. The second measure was related to the perceived intensity of vibrotactile flow. From each graph of time vs. perceived intensity, the variance of intensity values, denoted by β, was computed to evaluate the consistency of elicited sensation intensities.
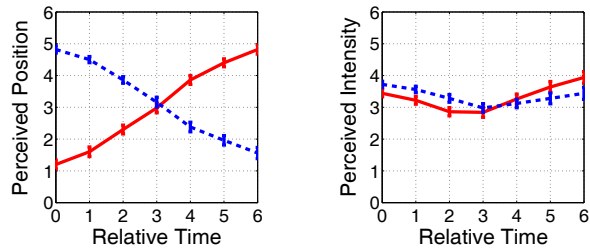
2.2 Results

For each vibrotactile flow, we averaged the graphs of the perceived position and intensity across trials and subjects. The results are shown in Figure 2.4, with the error bars representing standard errors.

In all plots of time vs. perceived position, it is evident that the perceived position of vibrotactile stimulation changed monotonically. The maximum amount of position variation was 3.62 level (= 4.827 cm in distance), and the minimum was 1.18 level (= 1.573 cm). We also tested the effects of the three independent variables (vibration rendering method, signal duration, and sensation movement direction) on the absolute values of the slope of fitted regression lines, α, via three-way ANOVA. It was shown that the vibration rendering method and the stimulation duration had statistically significant influences on α ($F(1,9) = 116.95, p < 0.0001$ and $F(1,9) = 5.79, p = 0.0395$, respectively), but the sensation movement direction did not ($F(1,9) = 0.16, p = 0.6974$).

Since the sensation movement direction was not a significant factor, we pooled the data of the upward and downward conditions, and obtained average α values for the four combinations of vibration rendering methods and signal durations. The results shown in Table 2.1 indicate that linear amplitude rendering produced vibrotactile flows that moved in a longer distance than log amplitude rendering under the same conditions. The grand means of α were 0.586 in linear amplitude rendering and 0.321 in log amplitude rendering, with a difference of 0.265. For signal duration, slower sensation movement ($T = 8$ s; corresponding velocity $= 1$ cm/s) resulted in larger α values than faster sensation movement ($T = 4$ s; corresponding velocity $= 2$ cm/s). The grand means of α were 0.505 for $T = 8$ s and 0.402 for $T = 4$ s, with a difference of 0.103. These results suggest that the vibration rendering method has more salient effects on the perceived distance of vibrotactile flow than the signal duration, at least in the tested range.
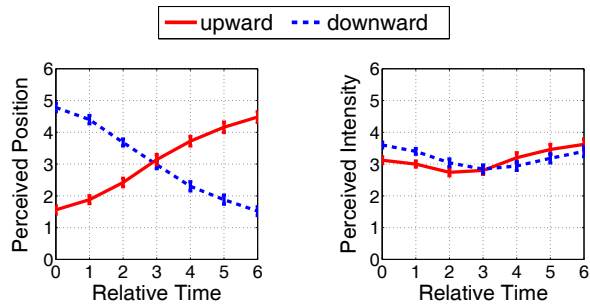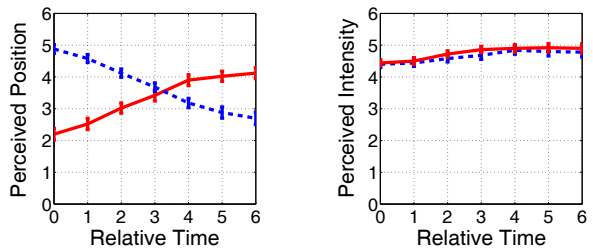
(a) Linear amplitude rendering and $T = 4$ s.

(b) Linear amplitude rendering and $T = 8$ s.
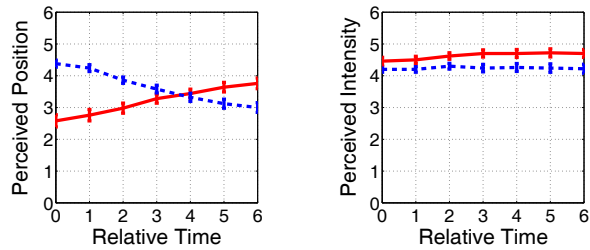
(c) Log amplitude rendering and $T = 4$ s.

(d) Log amplitude rendering and $T = 8$ s.

Figure 2.4: Experimental results. Relative time 0 and 6 indicate the beginning and ending time instants of a vibrotactile stimulus. Relative time 6 corresponds to 4 s in (a) and (c) and 8 s in (b) and (d).

Table 2.1: The absolute values of the fitted-line slopes of perceived position changes (α) and the variances of perceived intensities (β), both averaged across sensation movement directions and subjects.

Vibration Rendering Method	Signal Duration (s)	Average α	Average β
Linear amplitude	4	0.558	0.512
	8	0.614	0.641
Log amplitude	4	0.246	0.175
	8	0.396	0.306

The plots on the right in Figure 2.4 show the perceived intensities of vibrotactile flows. Three-way ANOVA verified that the vibration rendering method and the stimulation duration were statistically significant factors for β, the variance of perceived intensities ($F(1,9) = 9.03, p = 0.0148$ and $F(1,9) = 13.53, p = 0.0051$, respectively), but the sensation movement direction was not ($F(1,9) = 0.00, p = 0.9515$). It follows that, similarly to α, we computed average β values for the four combinations of vibration rendering methods and signal durations regardless of sensation movement directions, and showed them in Table 2.1.

According to the table, log amplitude rendering provided more consistent perceived intensities than linear amplitude rendering; the grand means of β were 0.577 for linear amplitude rendering and 0.246 in log amplitude rendering, with a difference of 0.331. In particular, linear amplitude rendering resulted in U-shaped curves in Figure 2.4, which means that vibration was perceived substantially weaker in the middle of the handheld mockup. In contrast, almost constant perceived intensities were observed for log amplitude rendering in Figure 2.4. Note that a similar phenomenon was reported for direct skin stimulation in the early haptics literature [20]. For stimulation duration, β was more consistent when vibrotactile flows moved faster ($T = 4$ s) than slower ($T = 8$ s). The grand means of β were 0.344 for $T = 4$ s and 0.479 for $T = 8$ s, with a difference of 0.135.

Similarly to α, the vibration rendering method was a more important factor for the consistency of perceived vibration intensities than the signal duration.

2.3   Discussion

The experimental results demonstrated that the sensation of vibrotactile flow can be reliably created in a mobile device using only two vibrotactile actuators. Among the three factors, different vibration rendering methods and signal durations significantly altered the perceptual characteristics of vibrotactile flows, but different stimulation movement directions did not. Linear amplitude rendering and slower sensation movements produced vibrotactile flows spanning in a longer distance than log amplitude rendering and faster sensation movements, respectively. This property can be useful in applications that require the high discriminability of sensation movement directions, especially under environments with other perceptual noises. In terms of the consistency of perceived intensity, log amplitude rendering and faster sensation movements showed better performance than linear amplitude rendering and slower sensation movements. Such smoothly moving vibrotactile sensations can be advantageous in some applications, e.g., those communicating affection. The trade-off should be carefully considered in designing a vibration rendering method and deciding associated parameters, depending on the goals of applications.

After the experiment, we directly attached the two LRAs on the palm without the device mockup. We could feel the phantom sensations, but they were substantially weaker than what could be produced with the mockup. Interestingly, it appears that the mockup greatly amplifies the sensations of vibrotactile flow. An investigation for this issue, including the modeling of vibration propagation dynamics in the mockup, is currently ongoing.

The vibrotactile flow adds a new dimension in designing vibrotactile effects

for a mobile device. First of all, it can increase the discriminability of tactons by allowing spatiotemporal information coding [9]. Also, the spatial property of vibrotactile flows is natural and intuitive, thus can greatly facilitate learning the associated meanings of tactons. Although not tested in this paper, the vibrotactile flow is expected to improve an information transmission rate, as observed in the early haptics literature for direct skin stimulation [20]. For actual applications, the vibrotactile flow can help produce realistic vibrotactile effects for mobile games, e.g., for shooting an arrow. It can also be used together with some GUI elements, such as a scroll bar, with an aim to enhance the inconvenience of the current GUI in a mobile device.

III. Perceptual Analysis of 1D Vibrotactile Flows

This chapter investigates the perceptual characteristics of vibrotactile flows rendered on a mobile device with a goal to find a synthesis framework of vibrotactile flows with desired perceptual properties. We uses synthesis equations of a general polynomial form extended from the amplitude inhibition algorithm presented in the previous chapter (Chapter II). we carried out a perceptual experiment to investigate the effects of the synthesis parameters on an expanded set of perceptual variables, including sensation movement distance, sensation velocity variation, sensation intensity variation, and the subjective confidence of flowlike sensation.

3.1 Perceptual Analysis Framework

3.1.1 Device

We used a mockup made of acrylic resin ($11\times6\times1$ cm; 82 g) to represent mobile devices. Two LRAs (LG Innotek; model MVMU-A360G; rated voltage 2.8 V (peak); nominal resonance frequency 175 Hz) were attached to the mockup, one at each end (10 cm apart), as shown in Figure 3.1. An LRA is an industry-standard variable reluctance actuator adopted in the vast majority of touchscreen mobile devices. It relies on the resonance of mass and spring elements to produce high-intensity vibrations with a fast response time. The two LRAs were powered by a custom-made amplifier connected to a PC via a data acquisition card (NI; PCI-6229) at a 10 kHz sampling rate.

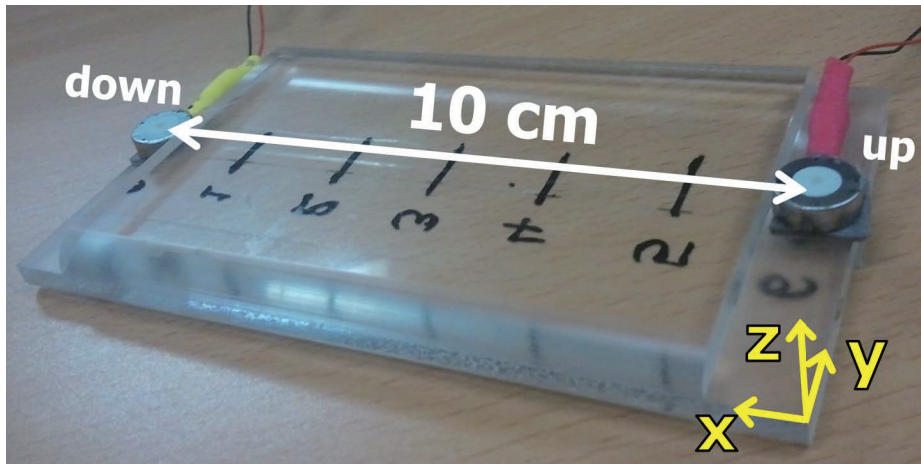To perceive vibrotactile flows from a mobile device, the most natural and

Figure 3.1: Mobile device mockup.

effective grasping posture is to enclose the device with a hand along the length direction, while maintaining close contact between the palm and the back panel of the device. In all experiments reported in this paper, users grasped the mockup in this posture, as also shown in Fig. 3.2.

To determine the drive frequency F, we estimated the frequency responses of the two LRAs using sinusoidal voltage inputs with frequencies in the range 1–500 Hz. The amplitudes of the resulting vibrations were measured using a high-precision accelerometer (Kistler; model 8765A250M5) that was fixed at the center of the mockup grasped in the experimenter's hand. The accelerometer responded to the z-axis vibrations (thickness direction; Fig. 3.1), since they matched the primary vibration direction of the LRAs. The estimated frequency responses are shown in Fig. 3.3. The two LRAs exhibited the same resonance frequency ($F = 178$ Hz), and this frequency was used for all the vibrotactile flows used in this work. Note that two vibration actuators driven with different frequencies produce low-frequency beats [24], which feel inherently different from smooth single-frequency vibrations [25]. In our experience, these beats impede the generation of clear vibrotactile flows.
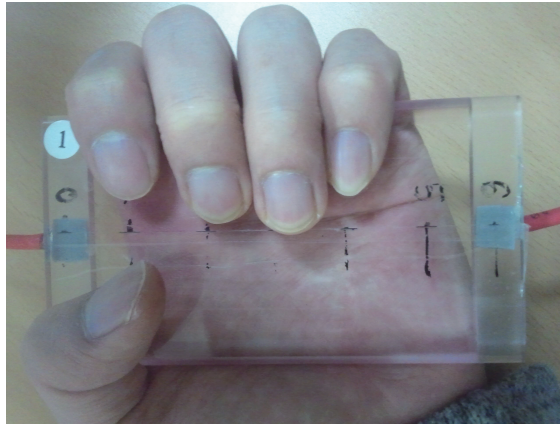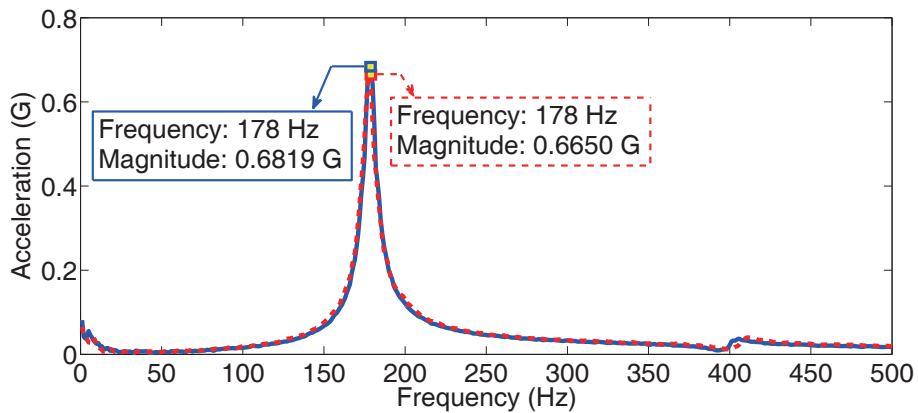
Figure 3.2: Grasping posture of the mockup.

Figure 3.3: Frequency responses of the two LRAs.

The next step was to calibrate the amplitude and phase characteristics of the two LRAs. The vibration amplitudes driven with $F = 178\,\mathrm{Hz}$ were measured for each LRA using the accelerometer for 20 input amplitude levels. The measured input-output relation was inverted for each LRA to determine the input voltage amplitude required to produce a desired output acceleration amplitude. Further, a non-zero phase offset existing between two sinusoidal waveforms reduces the superimposed amplitude of the two waves. Thus, we found a phase offset between the LRAs by exhaustively searching the phase difference between the two input waveforms that resulted in the largest output amplitude. This phase offset was $10\,^\circ$, and it was used in rendering all the vibrotactile flows used in our

experiments.

3.1.2 Synthesis Functions

Research has found three effective approaches for vibrotactile flow rendering: amplitude inhibition [14], time inhibition [13], and amplitude inhibition with a frequency sweep [15]. The time inhibition method modulates the onset timings of two vibrations and works well with ERMs [13]. In our experience, however, this technique is ineffective for producing clear flow sensations with LRAs. With the ERM that generally has correlated frequency-amplitude characteristics [26] and a long rising time, varying the input signal duration (much shorter than the rising time) also has the effect of changing the amplitude and frequency of the resulting vibration. However, such complication does not occur with LRAs. Moreover, the most recent approach in [15] enables the modulation of the spatial position at which vibratory resonance occurs on a device plate by combining amplitude inhibition with an input frequency sweep, but it requires the use of wideband actuators, which are still very rare in commercial mobile devices. Therefore, amplitude inhibition is the only viable option for LRAs.

The synthesis functions for vibrotactile flows we use are extended from the amplitude inhibition algorithm for phantom sensations presented earlier by Allies [20]. In our previous study [14], we tested two forms using linear and logarithmic functions, and they were shown to produce vibrotactile flows of different perceptual qualities on a mobile device. This result led us to consider the following general input synthesis equations:

$$a_1(t) = a_{max} \left(\frac{t}{T} \right)^{\gamma} \text{ and } a_2(t) = a_{max} \left(1 - \frac{t}{T} \right)^{\gamma}, \tag{3.1}$$

where $a_1(t)$ and $a_2(t)$ are the respective acceleration amplitudes that the two LRAs produce at time t, a_{max} is the maximum acceleration (1.17 G in our hardware setup), and T is the stimulus duration. With regards to t, these equations
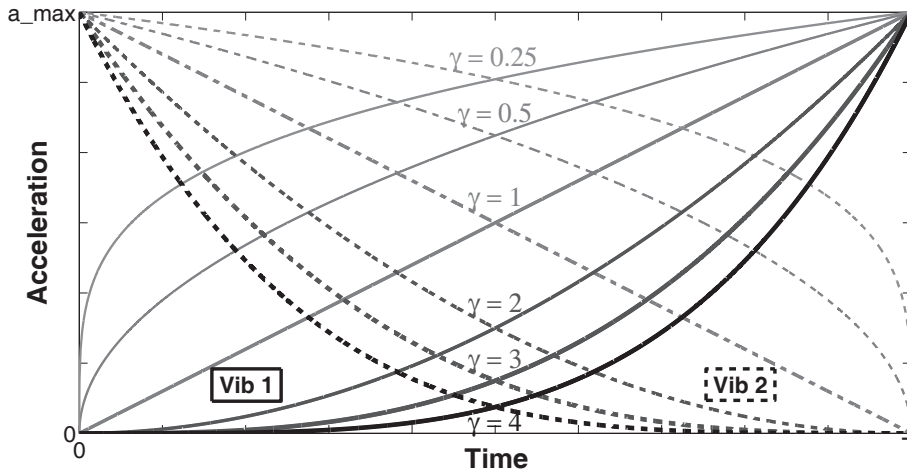
Figure 3.4: Vibrotactile flow synthesis functions.

are polynomials with a degree γ, which controls the shapes of the two functions, as depicted in Figure 3.4[1]. This synthesis rule was the best among the various other function forms we tested in terms of simplicity and capability for flow rendering.

To understand the relationship between the synthesis function and the vibration output, we measured the acceleration of vibrotactile flows at different positions on the device mockup. The measurement positions were on the centerline in the height direction. A sample result is provided in Figure 3.5, which shows that the vibration amplitude either decreased or increased over time, depending on the position. These spatiotemporal distribution of vibrotactile stimuli induces the phantom sensation that the vibration feels as if it is "flowing" from one end to the other end. Moreover, changing the parameters in (4.1) can bring systematic changes to the spatiotemporal distribution of vibrotactile stimuli, as illustrated in Figure 3.5, and subsequently to the perceptual quality of the vibrotactile flows.

---

[1]This use of "tactile gamma" is adapted from gamma correction that is popular in video and image systems [27].
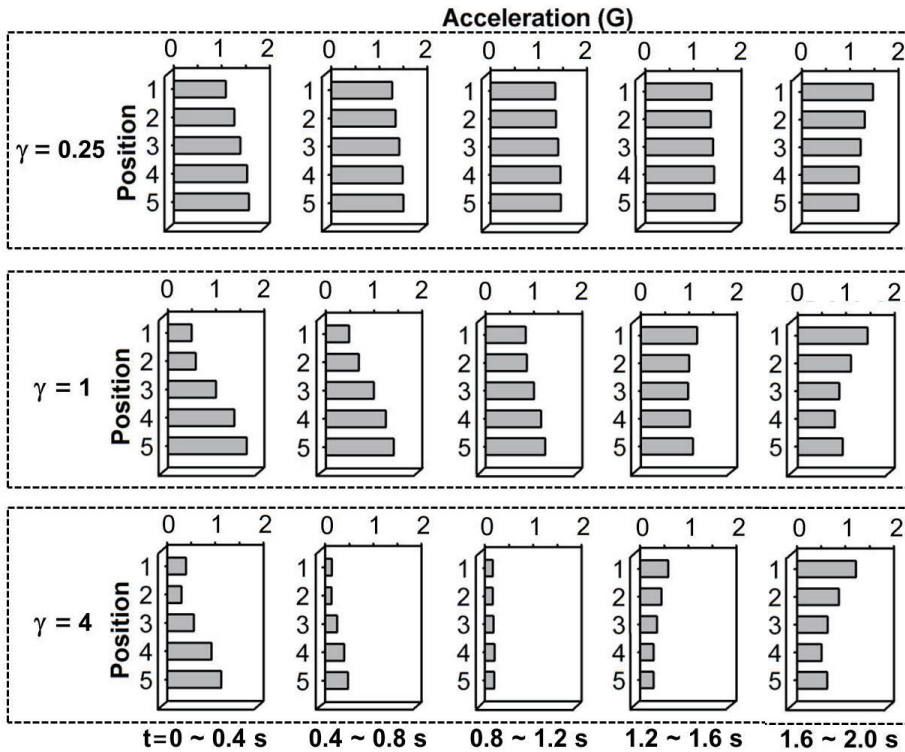
Figure 3.5: Spatiotemporal distributions of the acceleration amplitudes when vibrotactile flows were rendered through the mobile device mockup using the synthesis function in (4.1) with $T = 2$ s. During the measurements, the device mockup was grasped in the experimenter's hand, and the accelerometer was attached at the corresponding positions on the centerline on the front panel of the mockup
. Each plot shows the averages of 0.4 s measurements. Note that the position is a relative value.

3.2 Perceptual Characteristics

This section reports the perceptual experiment carried out to elucidate the effects of the synthesis function parameters on the perception of vibrotactile flow.

3.2.1 Methods

Participants

Fifteen volunteers (19–27 years old with an average 21.0; 9 males and 6 females; all right-handed) participated in this experiment. All participants were daily users of mobile phones with no known sensory impairments. They were paid at a rate of KRW 10,000 (about USD 9) per hour after the experiment.

Experimental Conditions

To render vibrotactile flows, we varied the two independent variables, γ and V. γ was selected from $\{0.25, 0.5, 1, 2, 4\}$, where the minimum and maximum values had ensured the sensation of movement in pilot experiments. V is the nominal velocity of sensation movement, and it also determines the duration T of vibrotactile flow by $V = 10 \, \text{cm}/T$, where $10 \, \text{cm}$ is the distance between the two LRAs. V was one of 3, 4, 7, 10, and $15 \, \text{cm/s}$, which correspond to T of 3.33, 2.5, 1.43, 1, and $0.67 \, \text{s}$, respectively. If $V > 15 \, \text{cm/s}$ ($T < 0.67 \, \text{s}$), the flow-like sensations are not salient, perhaps because of our perceptual limit, and the occasions for $V < 3 \, \text{cm/s}$ ($T > 3.33 \, \text{s}$) are rare in actual use. Combining the two independent variables resulted in 25 different vibrotactile flows.

Procedures

An open response paradigm was used in the experiment. The participant's task in each trial was to perceive a vibrotactile flow generated though the mockup grasped in their left hand and to draw two graphs to describe its perceptual characteristics with his/her right hand using the GUI-based program shown in Figure 3.6. The participants wore headphones that played white noise to block out any auditory cue.

First, the participant was asked to draw a graph for the position of the

vibration sensation vs. (relative) time. The time was represented in a seven-point scale from 0 to 6. The position was also shown in the same seven-point scale, but each interval was further divided into three segments. Thus, the participant could select a position from a total of 21 points between 0 and 6. This design was revised from our previous study, which used only seven points for the position, based on its questionnaire results [14]. Time levels 0 and 6 were defined as the beginning and ending times of the vibrotactile stimulation, respectively, and the position levels 0 and 6 as the positions of the LRAs at the bottom and top of the mockup, respectively. The gradation of the position was also marked on the device mockup. The participant was allowed to see the device mockup if it was necessary to compare the perceived position of a vibrotactile flow and the marked positions on the mockup. The participant could perceive the same vibrotactile flow repeatedly by pressing the "Vibration" button on the GUI.

Second, the participant drew another graph for the perceived intensity against time. The scales were the same as those of the position graph. A "Reference + Vibration" button on the GUI was used for this graph. Clicking this button produced a reference stimulus by vibrating the LRA at the bottom of the mockup for 1 s with an intensity of a_{max}, followed by the vibrotactile flow. The participant was instructed to regard intensity level 4 as the perceived intensity of the reference stimulus and intensity level 0 as that of no vibration and then to scale the perceived intensity of the vibrotactile flow accordingly, even in the case that the vibrotactile flow felt stronger than the reference stimulus.

Lastly, the participants rated their subjective confidence about having felt a "smooth and natural movement sensation" using a seven-point Likert scale (0–6).

The experiment began with a training session that consisted of 25 trials. During each trial, each participant completed the above task for one of the 25 vibrotactile flows. The order in which the 25 vibrotactile flows were presented
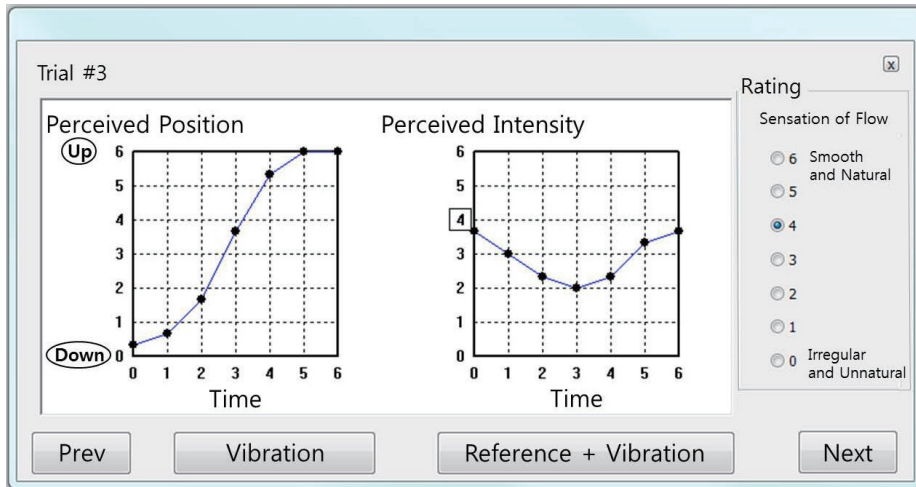
Figure 3.6: GUI of the program used for the perceptual experiment.

was randomized for each participant. The main session was essentially the same as the training session, except that each vibrotactile flow was repeated twice. Only the results of these 50 trials were used for data analysis. The participants had a 5-min break between the sessions. The experiment required about 1 h to complete for each participant.

Perceptual Measures

To represent the perceptual quality of vibrotactile flows, we defined four measures as follows: (1) *Sensation movement distance D*: The absolute difference of the perceived positions between time 0 and 6. This variable quantifies the perceived displacement of a vibrotactile flow. (2) *Sensation velocity variation Δ_v*: This measure gauges the perceived uniformity of vibrotactile flow movements. Let p_n $(0 \leq n \leq 6)$ be the perceived position at time n. For each graph of p_n and n, a best-fitting line $p = f(n)$ is found using linear regression. Then, $\Delta_v = \max_n |p_n - f(p_n)|$, indicating the maximum deviation of the perceived position from the linear movements. (3) *Sensation intensity variation Δ_i*: The difference between the maximum and minimum of the perceived intensities, representing
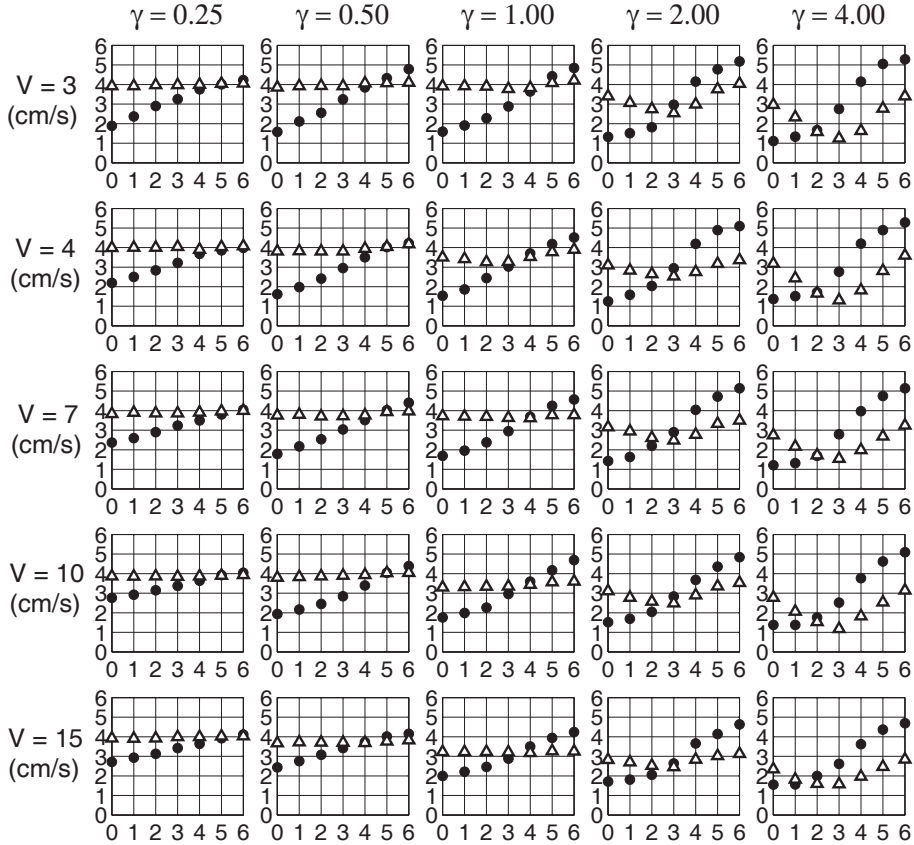
Figure 3.7: Plots of the perceived positions (filled circles) and the perceived intensities (unfilled triangles) (y-axis) vs. time (x-axis). Note that all are relative values.

the degree of perceived intensity changes. (4) *Confidence rating CF*: The rating of subjective confidence about "smooth and natural sensation movements." The more a vibration felt like a flow, the higher the participants rated CF.

3.2.2 Results

We averaged the graphs for the perceived position and intensity across participants for each experimental condition. The results are shown in Figure 3.7. In all the plots, it is evident that the perceived position of the vibrotactile flows changed monotonically.
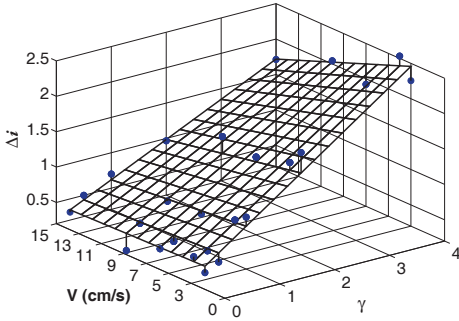
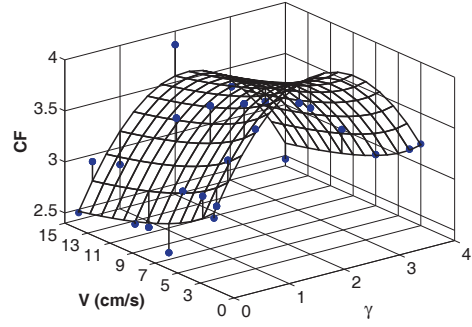The values of each of the four perceptual measures were computed from the
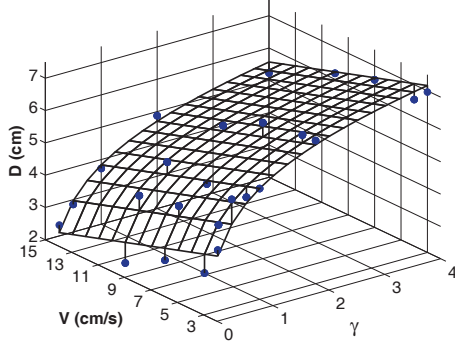
(a) Sensation movement distance D
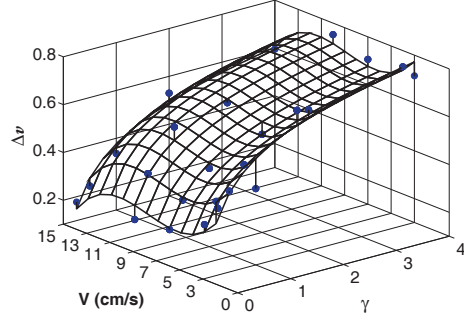
(b) Sensation velocity variation Δ_v

(c) Sensation intensity variation Δ_i

(d) Confidence rating CF

Figure 3.8: Perceptual measures vs. γ and V. For each measure, measured data and their best-fitting function are represented by circles and a meshed surface, respectively.

data in Figure 3.7, and they are provided in Figure 3.8. The data distribution of each measure passed the Shapiro-Wilk normality test with $p < 0.0001$. Thus, we performed a two-way ANOVA for each measure to examine the statistical significance of the two independent variables (γ and V) and their interaction. Then, mathematical functions that describe each perceptual measure with γ and V were found using the best subset regression. Details are reported below for each measure.

Sensation Movement Distance

The sensation movement distance D, shown in Figure 3.8(a), ranged from 2.13 to 6.96 cm. Considering that the distance between the two LRA was 10 cm,

this result indicates that the vibrotactile flows delivered clear movement sensations. Both γ and V had a statistically significant effect on D ($F(4, 56) = 27.85$, $p < 0.0001$ and $F(4, 56) = 11.58$, $p < 0.0001$, respectively), but their interaction did not ($F(16, 224) = 0.80$, $p = 0.6802$). The best-fitting regression model of D ($R^2 = 0.94$) was:

$$D = 1.25 \ \ln \gamma - 0.133 \ V + 5.83. \tag{3.2}$$

According to this equation, D increased logarithmically with γ, and it decreased linearly with V. γ controls the spatial rate of vibration intensity changes, and (3.2) suggests that γ is an effective indicator for the perception of sensation movement distance. V is responsible for the temporal rate of vibration intensity changes, but its effect on the sensation movement distance was weaker than that of γ.

Sensation Velocity Variation

The data of sensation velocity variation Δ_v are provided in Figure 3.8(b). Its values were distributed between 0.18 and 0.75, and $\max \Delta_v / \min \Delta_v = 4.23$, suggesting large differences of Δ_v. Both γ and V were statistically significant for Δ_v ($F(4, 56) = 32.14$, $p < 0.0001$ and $F(4, 56) = 5.51$, $p = 0.0008$, respectively), but their interaction was not ($F(16, 224) = 1.19$, $p = 0.2808$). The best-fitting model ($R^2 = 0.93$) was:

$$\Delta_v = 0.164 \ \ln \gamma - 0.000795 \ V^3 + 0.0211 \ V^2 - 0.172 \ V + 0.892. \tag{3.3}$$

Here, Δ_v increased logarithmically with γ. Given γ, Δ_v decreased, increased, and then decreased again with V in a third-order polynomial form. This complex behavior was due to the data points at $V = 7 \ \mathrm{cm/s}$, which formed local minima for all γ's. However, whether the differences in Δ_v around $V = 7 \ \mathrm{cm/s}$ are clearly perceptible to users in actual applications is questionable.

Sensation Intensity Variation

The sensation intensity variation Δ_i shown in Figure 3.8(c) varied between 0.12 and 2.53. As $\max \Delta_i / \min \Delta_i = 20.81$, the participants could reliably perceive the changes in the intensity. Both γ and V were statistically significant for Δ_i ($F(4, 56) = 96.76$, $p < 0.0001$ and $F(4, 56) = 4.79$, $p = 0.0022$, respectively), as well as their interaction ($F(16, 224) = 2.19$, $p = 0.0062$). The best-fitting function ($R^2 = 0.96$) was:

$$\Delta_i = 0.597\ \gamma - 0.0154\ \gamma V + 0.253. \qquad (3.4)$$

This model indicates that Δ_i increased linearly with γ, with a slope dependent on V. Δ_i decreased linearly with V, again with a slope dependent on γ.

Confidence Rating of Flow Sensation

The subjective ratings of the confidence of flow-like sensation, CF, are shown in Figure 3.8(d). The ratings ranged from 2.47 to 3.97 (neutral: 3). Both γ and V were statistically significant for CF ($F(4, 56) = 3.55$, $p = 0.0119$ and $F(4, 56) = 6.28$, $p = 0.0003$, respectively), but their interaction was not ($F(16, 224) = 1.34$, $p = 0.1756$). The best-fitting regression model ($R^2 = 0.82$) was:

$$CF = -0.290\ \gamma^2 + 1.27\ \gamma - 0.354\ \ln V + 3.14. \qquad (3.5)$$

Hence, CF initially increased with γ, reached the highest confidence at $\gamma \simeq 2$, and then began to decrease for $\gamma > 2$. CF was logarithmically decreased with V.

3.2.3 Discussion

The experimental results demonstrated that our synthesis function in (4.1) can effectively control the perceptual characteristics of a vibrotactile flow. The two synthesis parameters γ and V had statistically significant influence on all the

four perceptual metrics through well-defined functional relationships, which will be called perceptual characteristic functions in the remainder of this paper.

The exact equations for the perceptual characteristic functions would depend on the specific experimental setup. However, we expect that the general effects of γ and V on the four perceptual measures would remain intact. We actually tested different hardware setups by varying the distance between the two LRAs (3–10 cm) and the weight of the device mockup (100, 120, and 140 g), even on a thin plate (thickness < 0.2 cm). In all of these cases, the perceptual impression of vibrotactile flows was consistent with the patterns predicted by the perceptual characteristic functions. These results suggest that the perceptual characteristic functions can be applied to different hardware setups after simple scaling.

3.3 Applications

The perceptual characteristic functions describe how our perception of a vibrotactile flow is affected by the parameters of the synthesis function. Therefore, vibrotactile flows that have desired perceptual features can be designed using the inverses of the perceptual characteristic functions. For example, in applications that deliver the desired distance with directional information, the function for D in (3.2) can provide a reference for selecting appropriate vibrotactile flows. We actually implemented a bricks-breaking game (Arkanoid) in which the ball's movements and collisions are enhanced with vibrotactile flows. This game received quite positive responses in informal user tests. Likewise, the perceptual variable Δ_v or Δ_i can be essential for describing certain motions. In a golf game, for instance, the movement of a golf ball in the vertical direction may be reflected in the perceived velocity or intensity changes of a vibrotactile flow using (3.3) or (3.4), respectively. If the precise delivery of the direction of vibrotactile flow is of high priority, e.g., in navigation aids, the confidence rating CF in (3.5) deserves

more attention.

It should be remarked that the four perceptual measures are not independent of each other; they are determined by two independent variables γ and V. For example, our results suggest that it would be impossible to generate the vibrotactile flows that move in a short distance (low D) with high flow-like sensation (high CF). When D in Figure 3.8(a) is very low, the corresponding CF in Figure 3.8(d) is slightly less than 3 (the neutral score), indicating that the resulting vibrations could feel like a flow, but not very clearly. On the other hand, if large D is desired, Δ_v and Δ_i are also increased, while CF becomes low. This dependency between the four perceptual characteristic functions needs to be carefully taken into account for application design.

IV. Rendering of 2D Vibrotactile Flows: Edge Flows

This chapter addresses the following three research ploblems as to edge flows:

- **Information transmission capacity:** The spatiotemporal nature of edge flows was expected to improve the tactile information transmission capacity of the current mobile platform. The first aim of this study was to quantify the information transmission capacity of edge flows.

- **Learning effect:** We observed some need for learning, albeit short, for robust identification of 1D vibrotactile flows [14, 28], as also mentioned in the early studies on phantom sensations [20]. Our second goal was to assess the learning effect of edge flows, which was expected to be higher than for 1D flows.

- **Need for correct-answer feedback:** The last question pertains to the intuitiveness of edge flows; whether the learning requires correct-answer feedback. If practice without correct-answer feedback leads to performance improvement comparable to practice with feedback, it indicates that edge flows are sufficiently intuitive for users to learn by only trials and errors, without the needs for additional learning procedures or user interfaces.

To find answers to the three research problems, we designed 32 edge flows by changing their starting position, number of the 1D flows used, and rotation direction. Then users ability to identify the 32 edge flows was evaluated in a longitudinal user study (over a week). The experimental procedure on each day was designed such that the practice was similar to what one would experience in
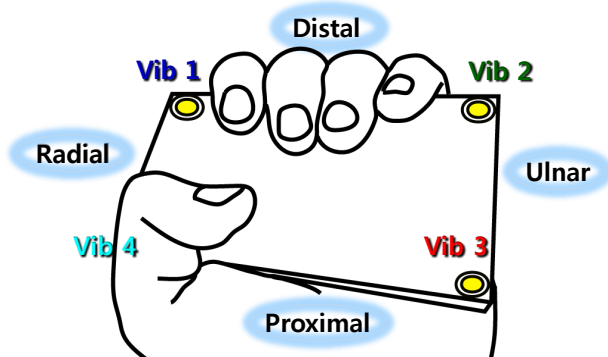
Figure 4.1: Mobile phone mockup and grasping posture used in the user study.

the daily use of a mobile device.

4.1 Methods

Our user study had three independent factors in a mixed-subjects design. Within-subjects factors were edge flow and day of practice, while a between-subjects factor was the use of correct-answer feedback. Details are presented below.

4.1.1 Edge Flows

Edge flows consist of multiple, concatenated 1D vibrotactile flows. Our design of edge flows assumed the use of four vibrotactile actuators each of which is placed at one of the four corners of a rectangular mobile device (Figure 4.1). The geometric path of an edge flow can be uniquely defined by its starting edge (SE; one of the four sides), the number of edges to span (NE; equal to the number of 1D flows to use), and rotation direction (RD; clockwise (CW) or counterclockwise (CCW)). By limiting NE $\leq$ 4, we designed 32 (4 SE$\times$4 NE$\times$2 RD) paths of edge flows, as shown in Figure 4.2.

Given an edge flow path, we also need to determine the algorithms to render individual 1D flows and their parameters. We use our synthesis algorithm of 1D
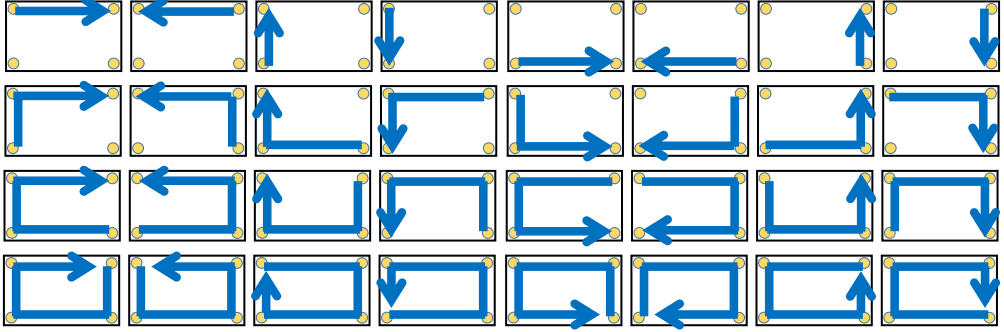
Figure 4.2: Geometric paths of 32 edge flows.

vibrotactile flows introduced in the previous chapter (Chapter III). This algorithm is based on amplitude inhibition and so suitable for LRAs. The synthesis equations for a 1D flow that progresses from LRA 1 to LRA 2 are:

$$a_1(t) = a_{max}\left(1 - \frac{t}{T}\right)^\gamma \text{ and } a_2(t) = a_{max}\left(\frac{t}{T}\right)^\gamma, \qquad (4.1)$$

where $a_1(t)$ and $a_2(t)$ are the respective accelerations that the two LRAs produce at time t, a_{max} is the maximum acceleration, and T is the stimulus duration. With regard to t, the two functions are polynomials with a degree γ. For the distance d between the two LRAs, $T = d/v$ where v is the nominal velocity of sensation movement.

Our previous study (Chapter III) showed that the two parameters, γ and v (or T), determine the perceptual characteristics of 1D vibrotactile flows, such as movement distance of a sensation, variation in the velocity or the intensity of a sensation, and the confidence of flow-like sensation. We could also find mathematical functions that can be used to design vibrotactile flows with desired perceptual properties. In order to render an edge flow, its constituent 1D flows are generated successively by driving the corresponding actuators using the synthesis equations in (4.1). An example is provided in Figure 4.3.

To render edge flows, we used a rectangular mobile phone mockup ($11\,\text{cm} \times 6\,\text{cm} \times 1\,\text{cm}$)
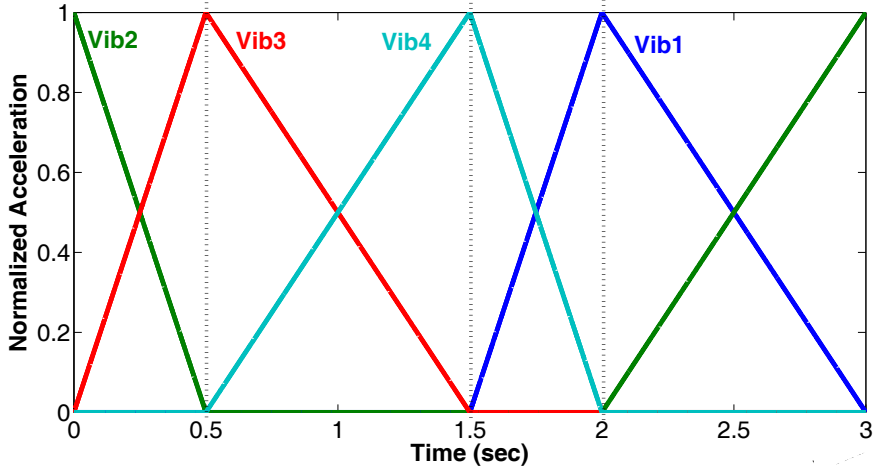
Figure 4.3: Input acceleration profile of the edge flow at the bottom-left corner of Figure 4.2. $\gamma = 1$. $T = 0.5\,\mathrm{s}$ for short edges and $1\,\mathrm{s}$ for long edges.

made of acrylic resin. Participants grasped the mockup with their non-dominant hand while enclosing the mockup with their palm and fingers (Figure 4.1). The short ends of the mockup were indented by $0.5\,\mathrm{cm}$. Four LRAs (LG Innotek MVMU-A360G) were attached at the four corners on the indented region to prevent direct contact of the LRAs to participants' hand. The center-to-center distance d between the LRAs was $10\,\mathrm{cm}$ along the long edges and $5\,\mathrm{cm}$ along the short edges. The LRAs were controlled by a PC at a sampling rate of $10\,\mathrm{kHz}$ using a data acquisition card (NI PCI-6723) and a power amplifier.

All the LRAs were driven at the same frequency ($177\,\mathrm{Hz}$). This frequency allowed us to use the greatest common amplitude for the LRAs according to their frequency responses. Note that using different frequencies create low-frequency beats [29], and it hinders rendering clear flow-like sensations [14, 28]. We also found the phase offset between each pair of the LRAs by exhaustively searching for the phase difference that resulted in the largest output amplitude. This was because a non-zero phase offset existing between two sinusoidal waveforms

reduces the superimposed amplitude of the two waves. Lastly, to produce desired acceleration amplitudes, the required input voltage amplitudes were obtained from a measured input-output relationship for each LRA. Further details of these calibration procedures are described in [28].

Other specific synthesis parameters were as follows: (1) $a_{max} = 0.36\,\text{G}$—the maximum amplitude that the four LRAs could commonly produce at $177\,\text{Hz}$ when the mockup was grasped in the hand, corresponding to about 35.44 dB SL using the absolute threshold taken from [26]; (2) $v = 10\,\text{cm/s}$—therefore $T = 1\,\text{s}$ on the long edges ($d = 10\,\text{cm}$) and $0.5\,\text{s}$ on the short edges ($d = 5\,\text{cm}$). The total durations of the edge flows varied between 0.5 and 3 s; (3) $\gamma = 1$—to provide vibrotactile flows with uniform perceived intensities and velocities over time [28].

4.1.2 Procedure

The experiment for each participant consisted of five practice sessions conducted on five consecutive days and one delayed recall test performed two or three days (depending on the participant's availability) after the practice.

Each practice session proceeded as follows. First, the participant was presented with the 32 edge flows, twice each, in the order shown in Figure 4.2 (left to right, then top to bottom). During the playback of each edge flow, a graphical user interface (GUI), which looked similar to Figure 4.2, highlighted the visual icon that represented the movement of the edge flow. The next edge flow started 2 s later to prevent tactile adaptation. Second, the participant went through 128 practice trials (32 edge flows×4 repetitions). On each trial, the participant perceived a randomly-selected edge flow, and then answered which edge flow was perceived by clicking the corresponding icon on the GUI program using a mouse. The participant could perceive the edge flow as many times as s/he needed. After the response, the correct answer was highlighted on the GUI program for visual

feedback. This feedback was optional depending on the condition to which the participant was assigned. Lastly, an immediate recall test followed, wherein the 32 edge flows were presented only once in a random order. The procedure was the same as that of the practice, except that no correct-answer feedback was given. One-day practice sessions were finished in approximately one hour.

The delayed recall test had the same procedure as the immediate recall tests in the practice sessions. It is noted that all the recall tests did not have repetitions, testing each edge flow only once. This was to make the recall tests as brief as possible; including repetitions in recall tests also provides practice to some extent.

Throughout the experiment, the participants wore noise-cancelling headphones to block the faint sound generated by the LRAs. The participants were allowed to take a break whenever necessary.

4.1.3 Participants

We recruited 20 participants for this experiment. Ten of them (five male and five female; 19–26 years old with a mean 20.7) were tested with no correct-answer feedback, while the other ten (five male and five female; 19–26 years old with a mean 21.8) were with correct-answer feedback. All of the participants were right-handed and daily users of a mobile phone. None of them reported known sensory impairment. The participants signed on a standard consent form prior to the experiment. They were paid KRW 10,000 (about USD 10) per hour after the experiment.

4.1.4 Performance Measures

We used the experimental data collected in the five immediate recall tests and the one delayed recall test for data analysis. For each recall test, the data of the ten participants measured under the same correct-answer feedback condition were

pooled to compute a stimulus-response confusion matrix. This confusion matrix was used to obtain the maximum likelihood estimate of information transfer IT using the standard formula [30]. This procedure results in only one IT for each recall test and correct-answer feedback condition.

IT represents how many bits of information the participants could identify from the 32 edge flows. IT is a unit-free measure of human performance that allows for comparisons across different modalities and displays [30]. 2^{IT} corresponds to the maximum number of edge flows that could be recognized without errors.

Another performance metric we used is the percent correct PC of each edge flow. Examination of PC enables us to find edge flows with high identifiability, and such knowledge is indispensable for the development of actual applications. However, PC is not appropriate for comparisons between different cases unlike IT. Even for the same stimuli, PC generally decreases with a larger stimulus set, but it does not necessarily imply that the total number of identifiable stimuli have decreased [31].

4.2   Results

4.2.1   Information Transfer

Figure 4.4 shows the values of IT measured in the five immediate recall tests after the practice of each day and the delayed recall test. Note that the maximum achievable IT was 5 bits (32 edge flows).

Without correct-answer feedback, IT increased with practice, and it was the greatest at the delayed recall test with IT = 3.39 bits and $2^{IT} = 10.5$. This improvement corresponds to 15% in IT and 36% in 2^{IT} compared to the lowest performance measured on day 1 (IT = 2.95 bits and $2^{IT} = 7.7$). With correct-answer feedback, IT also increased with practice in general, but the greatest value
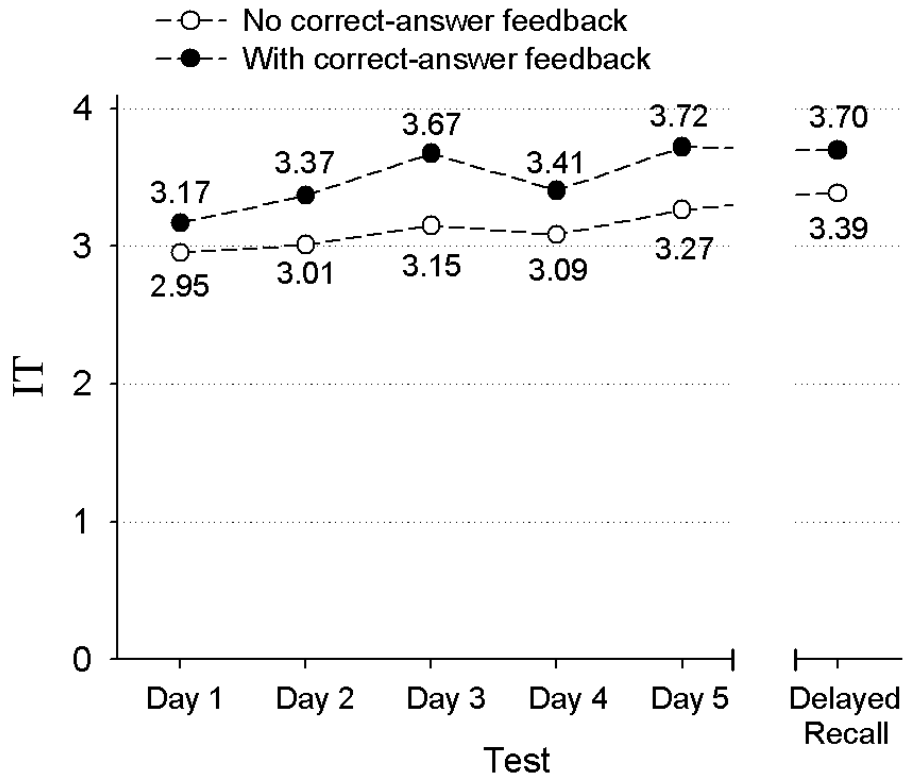
Figure 4.4: IT estimates measured in the immediate and delayed recall tests.

was measured on day 5 with IT = 3.72 bits and 2^{IT} = 13.2. The performance at the delayed recall test was slightly lower with IT = 3.70 bits and 2^{IT} = 13.0. This is an improvement of 17% in IT and 44% in 2^{IT} compared to the lowest performance of day 1 (IT = 3.17 bits and 2^{IT} = 9.0).

All IT values obtained with correct-answer feedback were higher than the corresponding ITs without correct-answer feedback. A two-sample t-test showed that the mean difference of IT between the two feedback conditions was statistically significant ($p = 0.0092$). Statistical tests for learning effect was not possible because only one IT value was available for each experiment day.
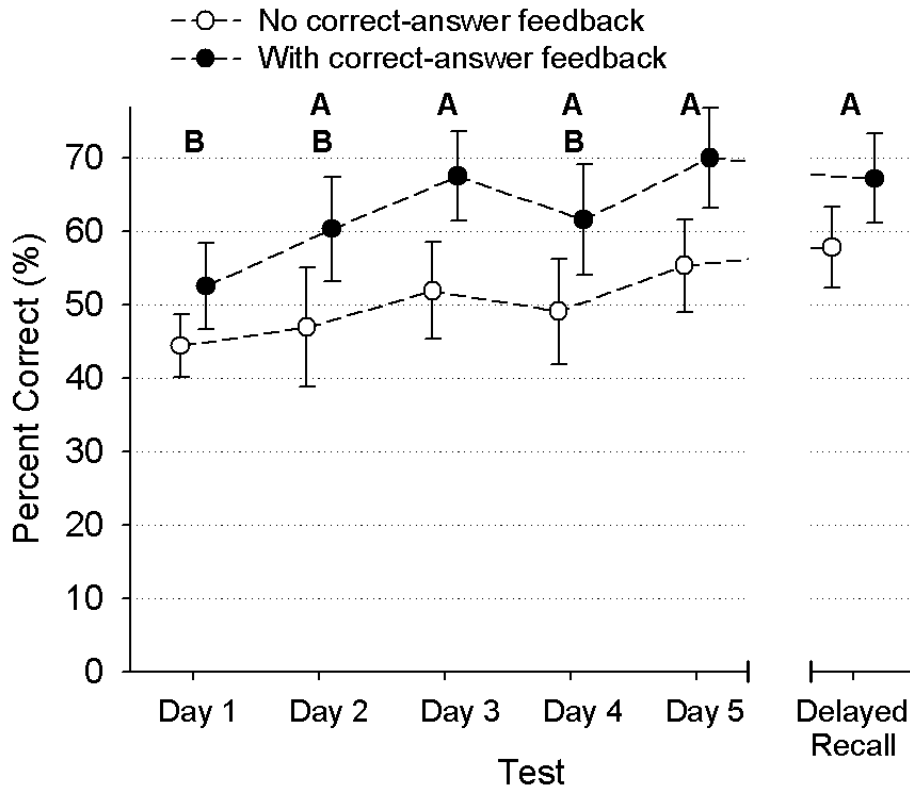
Figure 4.5: Percent correct scores. Error bars represent standard errors. Letters A and B indicate the results of a Tukey's HSD test for experiment day (A: a higher performance group and B: a lower performance group).

4.2.2 Percent Correct

Figure 4.5 shows the mean PC values averaged across edge flows and participants. The graphs exhibit similar trends to the graphs of IT in Figure 4.4. Without correct-answer feedback, the mean PC improved from 44.4% on day 1 to 57.8% at the delayed recall test. With correct-answer feedback, the mean PC increased from 52.5% on day 1 to 67.2% at the delayed recall test, with a maximum of 70% on day 5.

For each edge flow, the PC values of the ten participants who had a practice under the same correct-answer feedback condition were averaged for each experiment day. Then, we conducted a two-way mixed-design ANOVA on PC with

experiment day as a within-subjects factor and correct-answer feedback condition as a between-subjects factor. The effect of experiment day was statistically significant ($F(5, 90) = 3.03, p = 0.0143$). The effect of correct-answer feedback was not significant but close to the significance level ($F(1, 18) = 3.13, p = 0.0938$). We then performed a Tukey's HSD test for multiple comparisons to further investigate the effects of experiment day. The results are marked in Figure 4.5 using symbols, which indicate learning effects more clearly than the data of IT. The interaction term between the two factors was not significant ($F(5, 90) = 0.44, p = 0.8208$).

4.3   Discussion

4.3.1   Information Transmission Capacity

Our design of the 32 edge flows resulted in the highest IT of 3.70 bits at the delayed recall test after the participants had practiced for five days with correct-answer feedback. This value of IT means, at least theoretically, that we can recognize 13 edge flows with no errors.

The IT of our edge flows outperforms those reported in the following previous studies that used a single vibrotactile actuator: 1.76 bits—8 tactons that varied in amplitude, frequency, and pulse duration [7]; 2.5 bits—12 key-click signals with different amplitudes, frequencies, and the number of pulses [31]. The IT of our study is also higher than those reported earlier using multiple actuators: 1.99 bits—18 tactor locations of two 3×3 tactor arrays placed on the dorsal and volar sides of the wrist [32]; 1.90–2.49 bits—8 tactile patterns using 4 voice coil actuators around the wrist [33]; 2.46 bits—9 locations with a 3×3 motor array affixed to the palm [34]; 3.37 bits—27 tactons with different rhythms, roughnesses, and spatial locations using 3 voice coil actuators stimulating the forearm [35]. However, the IT of our edge flows was smaller than those reported in [12, 36]: 4.28 bits—24 vibration patterns generated using 3 vibration motors in a wrist-

band tactile display by changing their intensity, temporal pattern, starting point, and direction; 6.5 bits–120 stimuli using 4 finger configurations (thumb, index finger, middle finger, or all of them) and 30 waveforms with different frequencies and amplitudes. Note that accurate localization was enabled with those tactile stimuli.

The above comparisons indicate that the IT of edge flows is among the best that has been reported in the literature, even though edge flows do not require precise localization. We expect that the IT of edge flows can be further improved if other temporal factors, such as intensity, duration, and γ, are also considered in the design, similarly to [12].

4.3.2   Learning Effect

The performance improvement obtained by five-day practice was 15% in IT and 36% in 2^{IT} without correct-answer feedback, and it was 17% in IT and 44% in 2^{IT} with correct-answer feedback (Section 4.2.1). This can be regarded as a considerable learning effect, although formal statistical tests were not allowed for IT (only one value per condition). The learning effect manifested itself in the results of percent correct PC, for which the effect of practice was statistically significant (Section 4.2.2). In addition, examining Figure 4.4 and 4.5 suggests that the learning took place quickly; it could have reached a plateau as early as on day 3. Note that IT and PC on day 4 showed a decreasing tendency, but we are not certain of reasons at the moment.

Therefore, we can conclude that robust recognition of edge flows requires some practice, presumably due to their illusory nature. The learning can be done relatively quickly, however, possibly owing to their intuitive spatiotemporal characteristics.

4.3.3 Need for Correct-Answer Feedback

In terms of IT, providing correct-answer feedback during learning was helpful, leading to a statistically significant difference compared to the control condition of no correct-answer feedback (Section 4.2.1). As for PC, it was improved by correct-answer feedback, but not to the level of statistical significance, albeit the p-value (≈ 0.09) that approached significance (Section 4.2.2). At the delayed recall test, the extent of improvement enabled by correct-answer feedback was 9% in IT, 24% in 2^{IT}, and 16% in PC.

These results validate that correct-answer feedback is instrumental in improving the users' percent correct of edge flows. It is nonetheless worth mentioning that the performance improvement achieved by repeated practice was greater than that by correct-answer feedback.

4.3.4 Edge Flows with High Percent Correct Scores

In actual uses of edge flows, designers need to select the edge flows with the highest percept correct scores such that the number of selected edge flows is close to $2^{\text{IT}} = 13$. We selected such a set of edge flows using the method presented in [31]. We first sorted the 32 edge flows in a descending order of the mean PC measured in the delayed recall test. Beginning from the edge flow with the highest mean PC, we added each edge flow to the set one by one if the edge flow had low confusion rates with other edge flows already included in the set. The 13 best edge flows obtained in this way are shown in Figure 4.6. Stimuli chosen in this way retain the IT of the original stimulus set with almost perfect percent correct scores [31].

Then, we moved our attention to the means PCs for the three design variables measured in the delayed recall test (averaged between the two correct-answer feedback conditions), which are shown in Figure 4.7. The edge flows that start
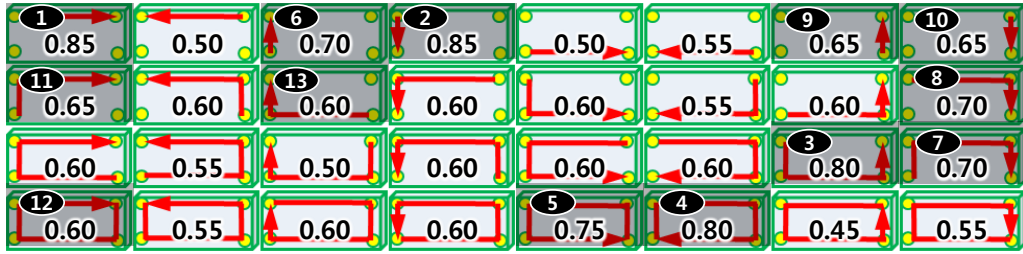
Figure 4.6: Mean PCs of individual edge flows measured in the delayed recall test. A number within each symbol represents the mean PC of the corresponding edge flow. The best 13 edge flows for uses in applications are highlighted and also ranked.
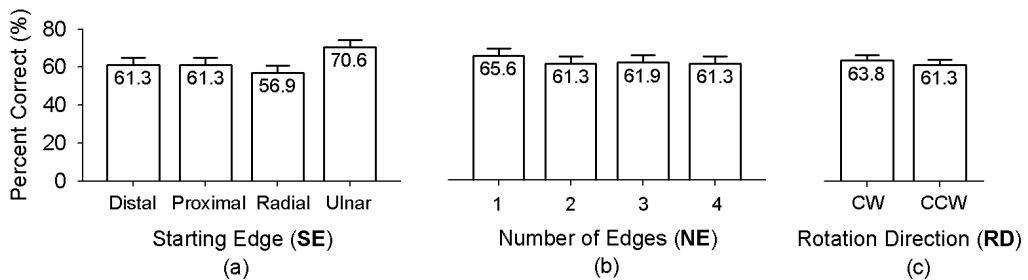

Figure 4.7: Means PCs measured in the delayed recall test for the three design variables of edge flows. Error bars represent standard errors.

at the ulnar side of the hand resulted in a substantially higher PC than the other edge flows (Figure 4.7(a)). The other three starting edges showed similar PCs. We are not aware of particular grounds for this behavior at the moment. As for the number of edges, $NE = 1$ showed the highest mean PC (Figure 4.7(b)), indicating that the simplest edge flows can be easier for identification than the other concatenated flows. The other edge flows with $2 \leq NE \leq 4$ resulted in similar PCs. Lastly, we were not able to find a noticeable difference in the mean PC between the two rotating directions of edge flows (Figure 4.7(c)). Note that we did not carry out further statistical analyses because of an insufficient number of data samples. Probing the effects of the three design variables of edge flows

can be an interesting topic for future research.

V.   Conclusion

In this thesis, we presented the design and results of a perceptual experiment that measured the performance of creating a linearly moving vibrotactile sensation on the user's palm holding a mobile device using only two vibrotactile actuators. The important contributions of this work can be summarized as: 1) Demonstration of the feasibility of the use of spatial vibrotactile stimulation for interaction with a mobile device and 2) Providing the trade-off in designing vibrotactile flows appropriate for the goals of applications.

In addition, ability of vibrotactile flows to produce diverse perceptual effects were studied. To this end, we used a polynomial-form synthesis function with two independent parameters of tactile gamma (the degree of the polynomial) and duration (or nominal movement velocity). The results of our perceptual experiment showed that these parameters can control the perceptual characteristics of vibrotactile flows in systematic manner.

Moreover, we have proposed to study edge flows as a first step to extend 1D vibrotactile flows to 2D. Edge flows consist of multiple, concatenated 1D vibrotactile flows rendered along the four edges of a rectangular mobile device using four actuators. We carried out a longitudinal user study over one week with 20 participants in order to investigate the information transmission capacity of edge flows, as well as the effects of practice and correct-answer feedback. The IT of edge flows was as high as 3.70 bits, being greater than the IT reported in the majority of previous studies pertaining to information transmission via the tactile sense. We found both repeated practice and correct-answer feedback beneficial for the improvement of edge flow identification. The learning could be done quickly in a few sessions, and repeated practice enabled higher performance

enhancement than correct-answer feedback. The contributions of this study can be summarized to: (1) the first proposal of edge flows as a means to improve the information transmission capacity of mobile devices and (2) a quantification of the benefits of repeated practice and correct-answer feedback for users' accurate recognition of edge flows.

요 약 문

진동 흐름이란 모바일 기기 표면 상에 연속적으로 움직이는 듯한 느낌 혹은 구현 방법을 일컫는다. 먼저 두 개의 진동자를 모바일 기기 상에 배치하였을 때 진동 흐름의 구현 가능성을 사용자 평가 실험을 통해 알아보았다. 이 실험에서 사용자는 인지되는 진동의 위치와 세기를 시간에 따라 그래프로 그렸다. 그 결과, 이러한 진동 흐름이 충분히 구현 가능한 것임을 확인할 수 있었으며, 더욱 부드럽고 명확한 진동 흐름을 위해서는 렌더링 방법과 지속 시간 간의 조율이 필요하다는 것을 알아내었다. 이를 바탕으로 진동 흐름의 인지적 특성을 파악하는 연구를 수행하였고, 원하는 인지적 특성을 갖춘 진동 흐름을 구현할 수 있는 제작 방법을 제안하였다. 이러한 1차원 상의 진동 흐름 연구에서 나아가서, edge flow 라는 네 개의 진동자를 직사각형의 코너에 배치하여 이를 따라 돌아가는 2차원 상의 진동 흐름의 연구로 확장하였다. 32개의 edge flow를 디자인하고 정보 전달량과 학습에 필요한 조건을 알아보기 위한 수일에 걸친 사용자 실험을 수행하였다. 그 결과 edge flow는 3.70 비트의 정보를 전달하는 것을 확인하였으며, 단기간의 연습으로 쉽게 학습이 되었다.

References

[1] Jane Hwang, Jaehoon Jung, Sunghoon Yim, Jaeyoung Cheon, Sungkil Lee, Seungmoon Choi, and Gerard J. Kim. Requirements, implementation, and applications of hand-held virtual reality. *International Journal of Virtual Reality*, 5(2):59–66, 2006.

[2] Eve Hoggan, Stephen A. Brewster, and Jody Johnston. Investigating the effectiveness of tactile feedback for mobile touchscreens. In *Proceeding of the SIGCHI Conference on Human Factors in Computing Systems*, pages 1573–1582. ACM, 2008.

[3] D. Wagner and D. Schmalstieg. First steps towards handheld augmented reality. In *Proceedings of the IEEE International Symposium on Wearable Computers*, pages 127–135, 2003.

[4] Eric Gunther. Skinscape: A tool for composition in the tactile modality. Master's thesis, Massachusetts Institute of Technology, 2001.

[5] Ronald T. Verrillo and George A. Gescheider. Perception via the sense of touch. In Ian R. Summers, editor, *Tactile Aids for the Hearing Impaired*, pages 1–36. Whurr Publishers Ltd, 19B Compton Terrace, London N1 2UN, England, 1992.

[6] Jonghyun Ryu, Chil-Woo Lee, and Seungmoon Choi. Improving vibrotactile pattern identification for mobile devices using perceptually transparent rendering. In *Proceedings of the International Conference on Human-Computer Interaction with Mobile Devices and Services (MobileHCI)*, pages 257–260. ACM, 2010.

[7] M. Azadi and L. Jones. Identification of vibrotactile patterns: Building blocks for tactons. In *Proceedings of the IEEE World Haptics Conference (WHC)*, pages 347–352, 2013.

[8] Karen E. MacLean. Foundations of transparency in tactile information design. *IEEE Transactions on Haptics*, 1(2):84–95, 2008.

[9] Eve Hoggan, Sohail Anwar, and Stephen A. Brewster. Mobile multi-actuator tactile displays. In *Lecture Notes on Computer Science (HAID 2007)*, volume LNCS 4813, pages 22–33, 2007.

[10] Alireza Sahami, Paul Holleis, Albrecht Schmidt, and Jonna Häkkilä. Rich tactile output on mobile devices. In *Proceedings of the European Conference on Ambient Intelligence*, pages 210–221, 2008.

[11] Seungmoon Choi and Katherine J. Kuchenbecker. Vibrotactile display: Perception, technology, and applications. *Proceedings of the IEEE*, 101(9):2093–2104, 2013.

[12] Seungyon "Claire" Lee and Thad Starner. Buzzwear: Alert perception in wearable tactile displays on the wrist. In *Proceedings of the ACM SIGCHI Conference on Human Factors in Computing Systems (CHI)*, pages 433–442, 2010.

[13] S.Y. Kim, J.O. Kim, and K. Kim. Traveling vibrotactile wave–A new vibrotactile rendering method for mobile devices. *IEEE Transactions on Consumer Electronics*, 55(3):1032–1038, 2009.

[14] J. Seo and S. Choi. Initial study for creating linearly moving vibrotactile sensation on mobile device. In *Proceedings of the Haptics Symposium*, pages 67–70. IEEE, 2010.

[15] J. Kang, J. Lee, H. Kim, K. Cho, S. Wang, and J. Ryu. Smooth vibrotactile flow generation using two piezoelectric actuators. *IEEE Transactions on Haptics*, 5(1):21–32, 2012.

[16] Sang-Youn Kim and Jeong Cheol Kim. Vibrotactile rendering for a traveling vibrotactile wave based on a haptic processor. *IEEE Transactions on Haptics*, 5(1):14–20, 2012.

[17] K. Yatani and K. N. Truong. SemFeel: A user interface with semantic tactile feedback for mobile touch-screen devices. In *Proceedings of the ACM Symposium on User Interface Software and Technology*, pages 111–120, 2009.

[18] Linda R. Elliott, Jan B.F. van Erp, Elizabeth S. Redden, and Maaike Duistermaat. Field-based validation of a tactile navigation device. *IEEE Transactions on Haptics*, 3(2):78–87, 2010.

[19] C. E. Sherrick and R. Rogers. Apparent haptic movement. *Perception & Psychophysics*, 1:175–180, 1966.

[20] David S. Allies. Information transmission by phantom sensations. *IEEE Transactions on Man-Machine Systems*, 11(1):85–91, 1970.

[21] S. Tachi, K. Tanie, K. Komiyama, K. Asaba, Y. Tomita, and M. Abe. Information transmission by two-dimensional electrocutaneous phantom sensation. In *Proceedings of the 8th Annual Northeast Bioengineering Conference*, pages 258–262, 1980.

[22] Ali Israr and Ivan Poupyrev. Tactile brush: Drawing on skin with a tactile grid display. In *Proceedings of the ACM SIGCHI Annual Conference on Human Factors in Computing Systems*, pages 2019–2028, 2011.

[23] Jongeun Cha, Lara Rahal, and A. E. Saddick. A pilot study on simulating continuous sensation with two vibrating motors. In *Proceedings of the IEEE*

International Workshop on Haptic Audio Visual Environments and their Applications, pages 143–147, 2008.

[24] Y. Yoo, I. Hwang, and S. Choi. Consonance perception of vibrotactile chords: A feasibility study. In *Lecture Notes on Computer Science (HAID 2011)*, volume LNCS 6851, pages 42–51, 2011.

[25] G. Park and S. Choi. Perceptual space of amplitude-modulated vibrotactile stimuli. In *Proceedings of the IEEE World Haptics Conference*, pages 59–64, 2011.

[26] J. Ryu, J. Jung, G. Park, and S. Choi. Psychophysical model for vibrotactile rendering in mobile devices. *Presence: Teleoperators and Virtual Environments*, 19(4):364–387, 2010.

[27] C. A. Poynton. *Digital video and HDTV: algorithms and interfaces.* Morgan Kaufmann, 2003.

[28] J. Seo and S. Choi. Perceptual analysis of vibrotactile flows on a mobile device. *IEEE Transactions on Haptics*, 6(4):522–527, 2013.

[29] Y. Yoo, I. Hwang, and S. Choi. Consonance of vibrotactile chords. *IEEE Transactions on Haptics*, 7(1):3–13, 2014.

[30] Hong Z. Tan, Charlotte M. Reed, and Nathaniel I. Durlach. Optimum information transfer rates for communication through haptic and other sensory modalities. *IEEE Transactions on Haptics*, 3:98–108, 2010.

[31] Hsiang-Yu Chen, Jaeyoung Park, Steve Dai, and Hong Z. Tan. Design and evaluation of identifiable key-click signals for mobile devices. *IEEE Transactions on Haptics*, 4(4):229–241, 2011.

[32] H. Chen, J. Santos, M. Graves, K. Kim, and H. Z. Tan. Tactor localization at the wrist. In *Lecture Notes in Computer Science*, volume 5024, pages 209–218, 2008.

[33] M. Matscheko, Johannes Kepler, Linz Linz, A. Ferscha, A. Riener, and M. Lehner. Tactor placement in wrist worn wearables. In *Proceedings of IEEE International Sympsoium on Wearable Computing (ISWC)*, pages 1–8, 2010.

[34] Katherine O. Sofia and Lynette A. Jones. Mechanical and psychophysical studies of surface wave propagation during vibrotactile stimulation. *IEEE Transactions on Haptics*, 6:320–329, 2013.

[35] Lorna M. Brown and Topi Kaaresoja. Feel who's talking: Using tactons for mobile phone alerts. In *CHI '06 Extended Abstracts on Human Factors in Computing Systems*, pages 604–609, 2006.

[36] Hong Z Tan, Nathaniel I Durlach, Charlotte M Reed, and William M Rabinowitz. Information transmission with a multifinger tactual display. *Perception & Psychophysics*, 61(6):993–1008, 1999.

Acknowledgements

Curriculum Vitae

Name   : Jongman Seo

Education

2005. 3. − 2009. 2.   Department of Computer Science and Engineering, Pohang University of Science and Technology (POSTECH) (B.S.)

2009. 3. − 2018. 8.   Department of Computer Science and Engineering, Pohang University of Science and Technology (POSTECH) (M.S.)